Eur. Phys. J. E **21**, 277–282 (2006)
DOI 10.1140/epje/i2006-10065-5

THE EUROPEAN PHYSICAL JOURNAL E

Effective triplet interactions in nematic colloids

M. Tasinkevych[1,2,a] and D. Andrienko[3]

[1] Max-Planck-Institut für Metallforschung, Heisenbergstrasse 3, 70569 Stuttgart, Germany
[2] Institut für Theoretische und Angewandte Physik, Universität Stuttgart, Pfaffenwaldring 57, 70569 Stuttgart, Germany
[3] Max-Planck-Institut für Polymerforschung, Ackermannweg 10, 55128 Mainz, Germany

Received 26 September 2006 and Received in final form 24 November 2006
Published online: 5 January 2007 –

Abstract. Three-body effective interactions emerging between parallel cylindrical rods immersed in a nematic liquid crystals are calculated within the Landau-de Gennes free-energy description. Collinear, equilateral and midplane configurations of the three colloidal particles are considered. In the last two cases the effective triplet interaction is of the same magnitude and range as the pair one.

PACS. 61.30.Dk Continuum models and theories of liquid crystal structure – 82.70.Dd Colloids – 61.30.Jf Defects in liquid crystals

1 Introduction

In colloidal suspensions knowledge of particle interactions is the key to understanding their thermodynamic properties. Typically it is assumed that the main contribution comes from the pairwise interactions between the particles. This simplifies the corresponding equations of motion which can then be solved using efficient numerical algorithms, such as molecular dynamics. However, in many systems the governing physical equations are nonlinear and this, in principle, can result in a modification of the interaction between two particles by the presence of other ones, meaning that the total interaction energy is no longer pairwise additive, and additional many-body potentials appear. The importance of many-body interactions has been recognized in a number of systems, from electron screening in metals [1], catalysis and island formation on surfaces [2], to charged colloids [3–7], binary mixtures [8], colloidal crystals [9,10] and simple liquids [11,12].

Attempts to characterize the solvent-mediated interactions have been made in case of nematic colloids [13–15], where colloidal particles experience long-ranged interactions mediated by the distortions of the nematic director around the particles [16–18]. These effective interactions result in particle clustering and self-organization [17,19]. Due to the presence of topological defects [20–24] the interparticle interaction is inherently anisotropic: depending on the symmetry of the director field around the particles either dipole-dipole or quadrupolar-type interactions can be observed [17,25].

The long-ranged nature of interactions mediated by the nematic director can result in a substantial many-body contribution to the interaction energy already for small concentrations of colloids. Indeed, recent theoretical studies of N-mers [26] and trimers [27] dispersed in a nematic host have shown that the three-body interactions can be of the same importance as two-body ones.

In spite of this fact, most research on nematic colloids still relies on pairwise-interaction potentials between the particles [28–32]. Moreover, often the director distribution around N particles is approximated by a superposition of one-particle solutions of a corresponding linearized theory (so-called Nicolson approximation), which yields vanishing many-body potentials. In addition, a linear superposition of one-particle solutions does not satisfy boundary conditions at all particle surfaces.

In this paper we would like to address the role of three-body interactions for long cylinders immersed in a nematic mesophase. This system can serve as a two-dimensional representation for nanoparticles in a nematic host. It is also a realistic model for carbon nanotubes-nematic liquid-crystal composites (discotic carbonaceous mesophases), which have recently been studied theoretically [26] and experimentally [33].

2 Many-body potentials and nematic free energy

Due to the anisotropic nature of the solvent, an analytical treatment of particle interactions is practically impossible already at a pairwise level. We therefore choose here a numerical approach: equations for the nematic order tensor

[a] e-mail: miko@fluids.mpi-stuttgart.mpg.de

are solved by minimizing the free energy numerically using finite elements with adaptive meshes [34]. For a system of N colloids at positions $\boldsymbol{r}_i$ we introduce an excess free energy F_N (defined below) over the free energy of a uniaxial nematic. F_N is then decomposed into effective n-body potentials $F^{(n)}$, with $n \leq N$, as follows [3]:

$$F_N = NF^{(1)} + \sum_{i<j}^{N} F^{(2)}(i,j) + \sum_{i<j<k}^{N} F^{(3)}(i,j,k) + \ldots, \quad (1)$$

where we introduce the shorthand notation for the center-of-mass positions $(\boldsymbol{r}_i, \ldots) \equiv (i, \ldots)$. The n-body potential is defined in the system with n colloidal particles. $F^{(1)} = F_1$ is the excess free energy coming from one isolated colloid. The effective pair interaction between two colloids follows from equation (1) when $N = 2$,

$$F^{(2)}(1,2) = F_2(1,2) - 2F_1. \quad (2)$$

The triplet potential $F^{(3)}(1,2,3)$ is defined in the system of three colloids, $N = 3$,

$$F^{(3)}(1,2,3) = F_3(1,2,3) - \sum_{i<j}^{3} F^{(2)}(i,j) - 3F_1. \quad (3)$$

By construction $F^{(3)}(1,2,3)$ tends to zero whenever one of the $r_{ij} \equiv |\boldsymbol{r}_i - \boldsymbol{r}_j| \to \infty$. $F^{(3)}(1,2,3)$ is the quantity we are interested in here.

The nematic host is modelled by the Landau-de Gennes free-energy density [35]

$$f = a(T - T^*)Q_{ij}Q_{ji} - bQ_{ij}Q_{jk}Q_{ki} + c\big(Q_{ij}Q_{ji}\big)^2 + \frac{L_1}{2}Q_{ij,k}Q_{ij,k} + \frac{L_2}{2}Q_{ij,j}Q_{ik,k}, \quad (4)$$

where Q_{ij} is the order parameter tensor, summation over repeated indices is implied and the comma indicates the spatial derivative. The positive constants a, b, c are assumed to be temperature independent, and T^* is the supercooling temperature of the isotropic phase. The constants L_1 and L_2 are related to the Frank-Oseen elastic constants $K_{11} = K_{33} = 9Q_b^2(L_1 + L_2/2)/2$, $K_{22} = 9Q_b^2L_1/2$, and Q_b is the bulk nematic order parameter. We introduce the dimensionless temperature $\tau = 24ca(T - T^*)/b^2$. The bulk nematic phase is stable for $\tau < \tau_{\rm NI} = 1$ with a degree of orientational order given by $Q_b = b(1 + \sqrt{1 - 8\tau/9})/8c$; $Q_b(\tau > 1) = 0$.

For the constants entering the free-energy density (4) we use typical values for a nematic compound 5CB [36,37]: $a = 0.044 \times 10^6\,\mathrm{J/m^3K}$, $b = 0.816 \times 10^6\,\mathrm{J/m^3}$, $c = 0.45 \times 10^6\,\mathrm{J/m^3}$, $L_1 = 6 \times 10^{-12}\,\mathrm{J/m}$, $L_2 = 12 \times 10^{-12}\,\mathrm{J/m}$, $T^* = 307\,\mathrm{K}$. The nematic-isotropic transition temperature for 5CB is $T_{\rm NI} = 308.5\,\mathrm{K}$. We choose $T = 308.3\,\mathrm{K}$, corresponding to $Q_b \approx 0.31$, close to the NI transition point, at which flocculation of colloidal particles, driven by attractive interactions, normally occurs. The nematic coherence length is $\xi = (24L_1c/b^2)^{1/2} \approx 10\,\mathrm{nm}$; it sets the smallest length scale in our system.

Three identical colloidal particles, each of which we take to be a long cylinder of radius R with the symmetry axis parallel to the z-axis, are immersed into a nematic liquid crystal. The order parameter at the system boundaries is fixed to the bulk order parameter of the nematic phase; the director orientation at the box boundaries is fixed along the y-axis. In this geometry the colloidal particles are orthogonal to the director field far from them (the other geometry is when the rods are aligned with the nematic). The problem of equilibrium orientation is discussed in reference [38].

The order parameter at the particle surfaces is fixed to the bulk order parameter. We consider fixed homeotropic boundary conditions at the particle surfaces, *i.e.* the director orientation is fixed along the surface normals.

Assuming translational symmetry of the system along the z-axis, the equilibrium distribution of the order parameter tensor Q_{ij} minimizes the free-energy functional $F = \int f \mathrm{d}x\mathrm{d}y$, where f is the free-energy density (4). The functional F is minimized numerically, using finite elements with adaptive meshing. The two-dimensional domain of integration of the free-energy density f is triangulated and the functions Q_{ij} are linearly interpolated within each triangle. Then the excess free energy F_N is calculated as

$$F_N = L_z \int (f - f_b)\mathrm{d}x\mathrm{d}y, \quad (5)$$

where $f_b = f(Q_b)$ and L_z is the length of colloidal particles. Here we will only talk about effective interactions per length, $\bar{F}_N = F_N/L_z$, $\bar{F}^{(n)} = F^{(n)}/L_z$. It will be understood that such scaling has been carried out, and we shall omit the overbars in the text below.

3 Results

3.1 Collinear geometry

In this case the three colloids are positioned on a line parallel to the nematic director $\boldsymbol{n}$, along the y-axis. Typical director orientation and order parameter maps are shown in Figure 1. Each particle is accompanied by two defect lines of strength $-1/2$, and the orientation of each defect pair is tilted with respect to the (fixed) director orientation far from the particles, Figure 1, left. Note that if a single colloidal particle is immersed in the nematic host, the accompanying defects will be positioned on a line perpendicular to the director orientation. The tilt angle (which breaks the mirror symmetry of the system) is a pure two-body effect and is already present in a system of two colloids [39]. At small separations, the three particles in a collinear geometry can serve as a model for a rod for which symmetry breaking has also been observed [40]. When the distance between the particles (1) and (2) is decreased (see Fig. 1, right), the orientation of the defects next to these particles tilts even more. However, this does not affect the order parameter and the director distribution around the third particle, *i.e.* one might anticipate

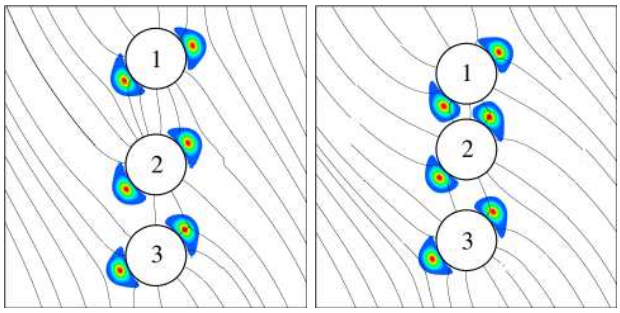

Fig. 1. (Color on-line) Order parameter and director distribution around colloidal particles with $R/\xi = 10$. Left: $r_{23} = 3R$, $r_{12} = 3.5R$; right: $r_{23} = 3R$, $r_{12} = 2.5R$. Director orientation far from the particles is parallel to the line connecting particle centers. Note that only a small part next to the particles is shown, the actual box size is $40R \times 40R$.

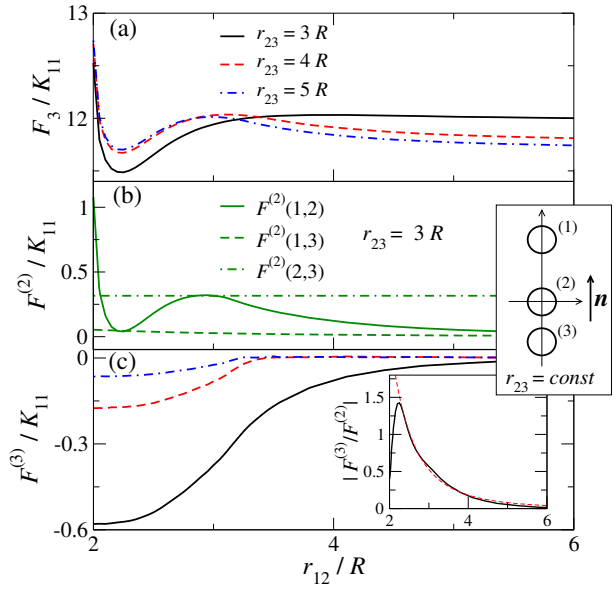

Fig. 2. (Color on-line) Collinear geometry. Three colloids are positioned on the line which is parallel to the director $\boldsymbol{n}$. Particle radius $R/\xi = 10$. (a) Excess free energy F_3 as a function of the separation between particles (1) and (2). The position of particle (3) is fixed with respect to particle (2) at $3R$, $4R$, and $5R$. (b) Pair potentials for $r_{23} = 3R$. (c) Three-body contribution to F_3; solid, dashed and dash-dotted lines correspond to $r_{23} = 3R$, $4R$ and $5R$, respectively. Inset shows the ratio between the three- and two-body contributions and a power law fit of the decaying tail for $r_{23} = 3R$.

that in a collinear geometry the contribution of the three-body potential to the total interaction energy is rather small, in line with the results of Guzmán *et al.* [27].

To assess this contribution, the total interaction energy F_3 as well as the pair $F^{(2)}$ and the triplet $F^{(3)}$ contributions to it are shown in Figure 2. Here we fix the distance between particles (2) and (3) at $3R$, $4R$, and $5R$ and study the interaction of these two particles with particle (1). The dependence of F_3 on separation r_{12} is similar for all three curves: particle (1) is repelled from particles (2) and (3) at large distances and there is a barrier which does not

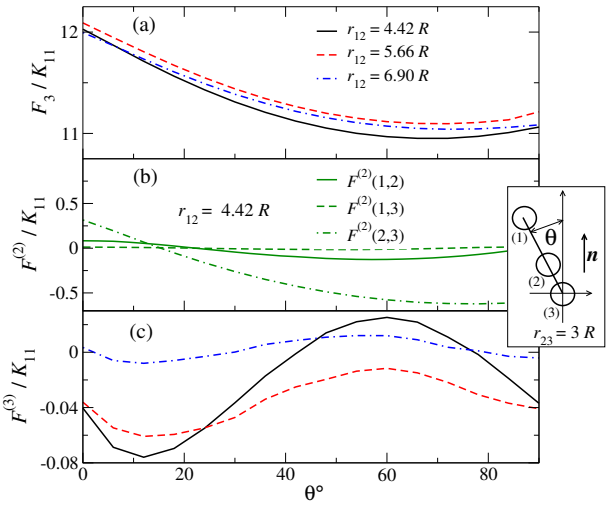

Fig. 3. (Color on-line) Collinear geometry, dependence on the tilt angle with respect to the nematic director: (a) excess free energy F_3; (b) two-body potentials; (c) three-body potential; solid, dashed and dash-dotted lines correspond to $r_{12} = 4.42R$, $5.66R$ and $6.90R$, respectively. Particle radius $R/\xi = 10$.

allow particle (1) to form a stable aggregate. The height of this barrier decreases with the decrease of the distance between particles (2) and (3). Figure 2b shows that the major contribution to the total interaction energy comes from the pairwise interaction of particles (1) and (2), especially at large separations of particles (2) and (3). However, for $r_{23} = 3R$ we have significant contribution of the three-body potential, which is shown in Figure 2c. In fact, this contribution is responsible for the decrease of the repulsive barrier and will lead to more efficient clustering of the colloids. For $r_{23} \lesssim 3R$ the pairs of defects around particles (2) and (3) start to tilt. The tilt angle increases with the decrease of r_{23}, affecting the effective interaction between the pair and the third colloid [41].

One can also see that in this geometry the three-body potentials always provide an attractive contribution to the total interaction energy. To emphasize the role of the three-body term, its ratio to the sum of two-body potentials is shown in the inset of Figure 2c for $r_{23} = 3R$. It clearly shows that at small separations, when rearrangement of the defects plays a major role, the three-body term is dominating and therefore, cannot be neglected. At larger distances the role of the three-body term becomes less important decaying as a power law $\mathcal{F}^{(3)}/\mathcal{F}^{(2)} \sim r_{12}^{-3.7}$.

We also study how the two contributions change under the director rotation. Figure 3 shows the tilt angle dependence of the excess free energy F_3, as well as two- and three-body contributions to it. It is interesting that our calculations predict an equilibrium configuration with a tilt angle about 70° with respect to the nematic director, *i.e.* there is also a torque acting on the line of colloids. The tilt is due to the pairwise interactions: the three-body contribution, in fact, has a *maximum* at about 60° and favors almost collinear with the director alignment (minimum at about 10°).

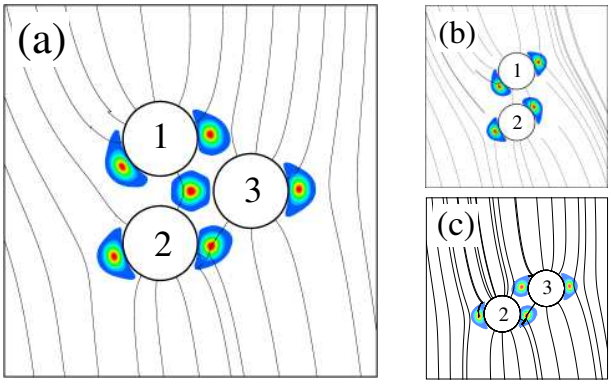

Fig. 4. (Color on-line) Order parameter and director distribution for the case of equilateral-triangle geometry, $r_{12} = r_{13} = r_{23} = 2.8R$, $R/\xi = 10$. (a) Three particles; (b) the same geometry, but particle (3) is removed; (c) particle (1) is removed. The director far from the particles is parallel to the line connecting the centers of particles (1) and (2). Only a small area next to the particles is shown.

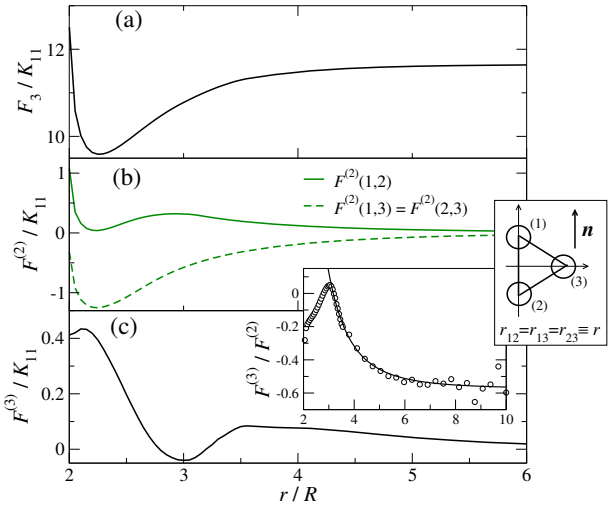

Fig. 5. (Color on-line) Equilateral-triangle geometry, $R/\xi = 10$. (a) Total interaction energy F_3; (b) two-body contributions; (c) three-body contribution. Inset shows the ratio between the three- and two-body contributions and a power law fit ($r^{-3.5}$) of the tail.

3.2 Equilateral-triangle geometry

The order parameter and the effective interaction potentials for the equilateral-triangle geometry are presented in Figure 4 and Figure 5, respectively. Already the director and order parameter profiles, depicted in Figure 4, show that the three-body potential is significant in this case: the position of the defects and the director orientation around three colloids (see Fig. 4a) cannot be obtained as a superposition of the corresponding two-particles profiles (see Figs. 4b and c), even at large separations. Since in the equilateral triangle geometry defect structures are less separated than in the collinear one, a much stronger three-body contribution is expected in this case.

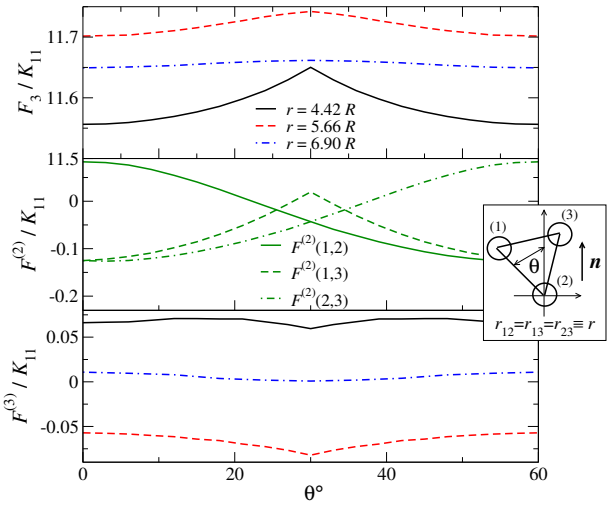

Fig. 6. (Color on-line) Equilateral-triangle geometry, tilt angle dependence of the effective interaction energies. $R/\xi = 10$. Bottom panel: solid, dashed and dash-dotted lines correspond to $r = 4.42R$, $5.66R$ and $6.90R$, respectively.

In Figure 5a F_3 as a function of the triangle size r is shown, demonstrating attraction of the particles at large r. Pairwise contributions show that particles (1) and (2) repel each other at large distances, while the particles of pairs (2)-(3) and (1)-(3) attract each other. The three-body contribution is almost always positive, and has a minimum around $r = 3R$. Contrary to the collinear geometry, the ratio $F^{(3)}/F^{(2)}$, which is shown in the inset of Figure 5, does not vanish at large r. Moreover, it converges to a constant (negative) value. This means that at large distances the three-body potential decays with the same power law as the two-body ones. Therefore, it cannot be neglected even at large separations between the colloidal particles.

The effective interaction potentials reveal rather weak dependence on the tilt angle, which is shown in Figure 6. The peaks around 30° are related to the defect rearrangement around the particles.

3.3 Midplane geometry

In this geometry the position of particle (3) is fixed at a distance x_3 from the line connecting particles (1) and (2) (the geometry is depicted in Fig. 7). The addition of the third particle changes the repulsive interaction between particles (1) and (2) to the attractive one, favoring their flocculation. The $F^{(3)}/F^{(2)}$ ratio shows the same tendency as in the equilateral-triangle case: it does not reach zero at large r_{12}, *i.e.* the three-body potential is long-ranged and provides about 10% correction to the sum of pair potentials at all distances.

3.4 Four-body interactions

To get the feeling of the next (four-body) term in expansion (1) we considered a system of four colloidal particles

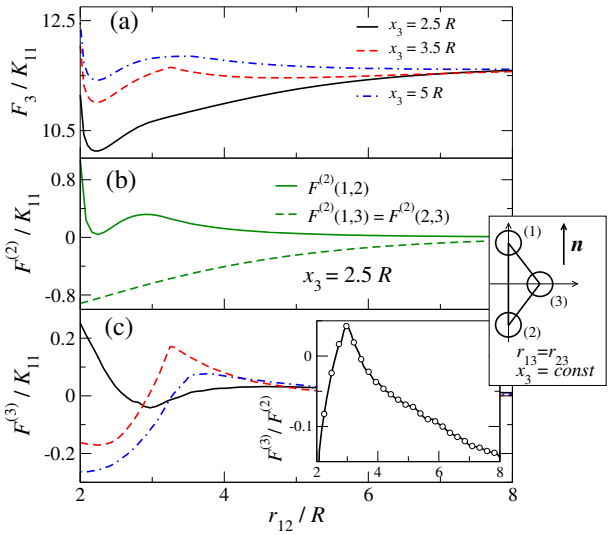

Fig. 7. (Color on-line) Midplane geometry, $R/\xi = 10$: (a) total interaction energy; (b) pairwise contributions; (c) three-body contribution; solid, dashed and dash-dotted lines correspond to $x_3 = 2.5R$, $3.5R$ and $5R$, respectively. Inset shows the ratio between the three- and two-body contributions for $x_3 = 2.5R$.

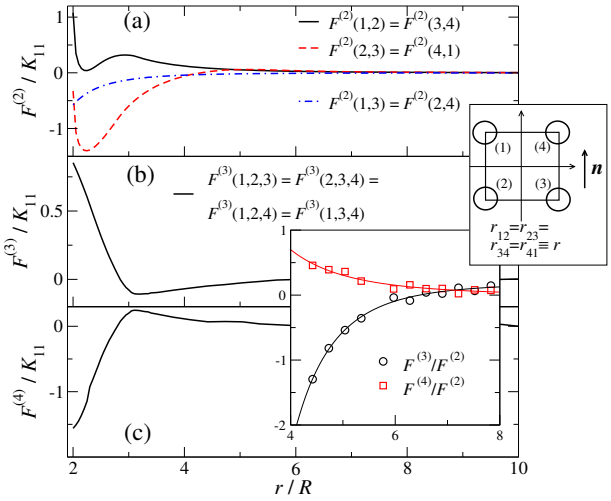

Fig. 8. (Color on-line) Effective interaction potentials for four colloidal particles in a square geometry, with $R/\xi = 10$. (a) Pairwise contributions; (b) three-body contributions; (c) four-body contribution. Inset shows the ratio between the three-, four- and two-body contributions with the power law fits.

positioned at the vertices of a square. Two-, three-, and four-body potentials are shown in Figure 8. The inset shows the ratio of the total three- and four-body contributions to the two-body one. The total two- and three-body contributions to F_4 are calculated as follows:

$$F^{(2)} = 2\left[F^{(2)}(1,2) + F^{(2)}(2,3) + F^{(2)}(1,3)\right],$$
$$F^{(3)} = 4F^{(3)}(1,2,3).$$

Fitting the ratios $F^{(i)}/F^{(2)}$ $(i = 3, 4)$ to the power law $(a_i/x)^{\gamma_i} + b_i$ in the region $r \in [6R \ldots 10R]$ yields $\gamma_3 = 5.5$, $b_3 = 0.18$ and $\gamma_4 = 3.6$, $b_4 = -0.01$. Again, at short distances the contribution of the three-body potentials to F_4 is comparable to the contribution of the two-body potentials. Moreover, the fit shows that both contributions have the same range and that three-body potentials amount up to 10% of the two-body terms even at large separations. The four-body term is slightly smaller than the three-body one. However, the slow convergence of expansion (1) does not allow to make a quantitative estimate of a many-body contribution that can be neglected.

4 Conclusions

Our calculations indicate that a collinear array of colloids (in our case modelled as infinitely long rods) is not as stable as the equilateral-triangle configuration. The most stable equilateral-triangle configuration is when one of the sides of the triangle is parallel to the nematic director.

Russ *et al.* [3] have shown that the triplet interaction is a function of the summed distance $r_{12} + r_{23} + r_{31}$ between the three particles only. However, this empirical observation does not hold in our case. The possible reasons are: anisotropic nature of the interactions and presence of topological defects, both of which are absent in a system of charged colloids.

The main message of this work is that in nematic colloids many-body effects cannot be neglected. At short distances rearrangements of accompanying defects strongly contribute to the three- and four-body terms in the free-energy expansion. In some geometries (*e.g.* equilateral triangle) the exponents of the power law decay of the two- and three-body contributions with interparticle distance are the same, *i.e.* the higher-order contributions cannot be neglected even at large separations.

Comments, remarks, and discussions with Markus Deserno are greatly acknowledged.

References

1. J. Hafner, *From Hamiltonians to Phase Diagrams* (Springer, Berlin, 1987).
2. L. Österlund, M.O. Pedersen, I. Stensgaard, E. Lægsgaard, F. Besenbacher, Phys. Rev. Lett. **83**, 4812 (1999).
3. C. Russ, H.H. von Grünberg, M. Dijkstra, R. van Roij, Phys. Rev. E **66**, 011402 (2002).
4. M. Brunner, J. Dobnikar, H.-H. von Grünberg, C. Bechinger, Phys. Rev. Lett. **92**, 078301 (2004).
5. C. Russ, M. Brunner, C. Bechinger, H.H. von Grünberg, Europhys. Lett. **69**, 468 (2005).
6. M. Dijkstra, R. van Roij, A.A. Louis, H.H. von Grünberg, preface to the special issue dedicated to *The CECAM Workshop: Effective Many-Body Interactions and Correlations in Soft Matter*, J. Phys.: Condens. Matter, Vol. **15**, no. 48 (2003).
7. A.-P. Hynninen, M. Dijkstra, R. van Roij, J. Phys.: Condens. Matter **15**, S3549 (2003).
8. S. Amokrane, A. Ayadim, J.G. Malherbe, J. Phys.: Condens. Matter **15**, S3443 (2003).

9. J. Dobnikar, Y. Chen, R. Rzehak, H.H. von Grünberg, J. Chem. Phys. **119**, 4971 (2003).
10. J. Dobnikar, Y. Chen, R. Rzehak, H.H. von Grünberg, J. Phys.: Condens. Matter **15**, S263 (2003).
11. C. Russ, K. Zahn, H.H. von Grünberg, J. Phys.: Condens. Matter **15**, S3509 (2003).
12. K. Zahn, G. Maret, C. Russ, H.H. von Grünberg, Phys. Rev. Lett. **91**, 115502 (2003).
13. R.W. Ruhwandl, E.M. Terentjev, Phys. Rev. E **55**, 2958 (1997).
14. T.C. Lubensky, D. Pettey, N. Currier, H. Stark, Phys. Rev. E **57**, 610 (1998).
15. D. Andrienko, M. Tasinkevych, P. Patrício, M.P. Allen, M.M. Telo da Gama, Phys. Rev. E **68**, 051702 (2003).
16. S. Ramaswamy, R. Nityananda, V.A. Raghunathan, J. Prost, Mol. Cryst. Liq. Cryst. Sci. Technol. Sect. A-Mol. Cryst. Liq. Cryst. **288**, 175 (1996).
17. P. Poulin, H. Stark, T.C. Lubensky, D.A. Weitz, Science **275**, 1770 (1997).
18. M. Yada, J. Yamamoto, H. Yokoyama, Phys. Rev. Lett. **92**, 185501 (2004).
19. V.J. Anderson, E.M. Terentjev, S.P. Meeker, J. Crain, W.C.K. Poon, Eur. Phys. J. E **4**, 11 (2001).
20. E.M. Terentjev, Phys. Rev. E **51**, 1330 (1995).
21. O.V. Kuksenok, R.W. Ruhwandl, S.V. Shiyanovskii, E.M. Terentjev, Phys. Rev. E **54**, 5198 (1996).
22. R.W. Ruhwandl, E.M. Terentjev, Phys. Rev. E **56**, 5561 (1997).
23. H. Stark, Eur. Phys. J. B **10**, 311 (1999).
24. D. Andrienko, G. Germano, M.P. Allen, Phys. Rev. E **63**, 041701 (2001).
25. J.C. Loudet, P. Poulin, Phys. Rev. Lett. **87**, 165503 (2001).
26. G. Gupta, A.D. Rey, Phys. Rev. Lett. **95**, 127802 (2005).
27. O. Guzmán, N.L. Abbott, J.J. De Pablo, J. Polym. Sci. Part B: Polym. Phys. **43**, 1033 (2004).
28. B.I. Lev, P.M. Tomchuk, Phys. Rev. E **59**, 591 (1999).
29. J.-ichi Fukuda, B.I. Lev, K.M. Aoki, H. Yokoyama, Phys. Rev. E **66**, 051711 (2002).
30. S.B. Chernyshuk, B.I. Lev, H. Yokoyama, Phys. Rev. E **71**, 062701 (2005).
31. D. Andrienko, M. Tasinkevych, S. Dietrich, Europhys. Lett. **70**, 95 (2005).
32. D. Andrienko, M. Tasinkevych, P. Patrício, M.M. Telo da Gama, Phys. Rev. E **69**, 021706 (2004).
33. J.E. Zimmer, R.L. Wetz, in *Extended Abstracts of the 16th Biennial Conference on Carbon (1983)* (American Carbon Society, University Park, PA, 1983) p. 92.
34. O.C. Zienkiewicz, R.L. Taylor, J.Z. Zhu, *The Finite Element Method: Its Basis and Fundamentals*, 6th edition (Butterworth-Heinemann, Oxford, 2005).
35. P.G. de Gennes, J. Prost, *The Physics of Liquid Crystals* (Clarendon Press, Oxford, 1995).
36. H.J. Coles, Mol. Cryst. Liq. Cryst. **49**, 67 (1978).
37. S. Kralj, S. Žumer, D.W. Allender, Phys. Rev. A **43**, 2943 (1991).
38. S.V. Burylov, Y.L. Raikher, Phys. Rev. E **50**, 358 (1994).
39. N.M. Silvestre, P. Patrício, M. Tasinkevych, D. Andrienko, M.M. Telo da Gama, J. Phys.: Condens. Matter **16**, S1921 (2004).
40. D. Andrienko, M.P. Allen, G. Skacej, S. Zumer, Phys. Rev. E **65**, 041702 (2002).
41. M. Tasinkevych, N.M. Silvestre, P. Patrício, M.M. Telo da Gama, Eur. Phys. J. E **9**, 341 (2003).